https://doi.org/10.5194/nhess-2019-200
Preprint. Discussion started: 28 June 2019

Natural Hazards and Earth System Sciences
Discussions

Towards an Automatic Early Warning System of Flood Hazards based on Precipitation Forecast: The case of the Miño River (NW Spain)

José González-Cao, Orlando García-Feal, Diego Fernández-Nóvoa, José Manuel Domínguez-Alonso, Moncho Gómez-Gesteira

Environmental Physics Laboratory (EPhysLab), CIM-UVIGO
Universidade de Vigo
Ourense, Spain

Correspondence to: D. Fernández-Nóvoa (diefernandez@uvigo.es)

Abstract: An Early Warning System for flood prediction based on precipitation forecast is presented. The system uses rainfall forecast provided MeteoGalicia in combination with a hydrologic (HEC-HMS) and a hydraulic (Iber+) models. The upper reach of the Miño River and the city of Lugo (NW Spain) are used as a study area. Starting from rainfall forecast, HEC-HMS calculates the streamflow and Iber+ is automatically executed when a certain threshold is exceeded for some previously defined risk areas. The analysis based on historical extreme events shows that the system can provide accurate results in less than one hour for a forecast horizon of 3 days and report an alert situation to decision-makers.

1. Introduction

According to Noji (2000), floods are one of the most dangerous natural hazards in the world. Jonkman (2005) estimates that more than 100,000 deaths in the last century were caused by floods. From 1940 to 2018 the number of deaths related with flood events (8138) is only surpassed by the lightning fatalities (9386) in the U.S. (https://www.nws.noaa.gov/om/hazstats.shtml). Furthermore, the effect of the Climate Change will increase the number of flood events and their negative impact to people and properties (Dankers and Feyen, 2008; Alfieri et al., 2017). Therefore, the ability to predict these extreme events and prevent their consequences is a challenge for the scientific community worldwide.

https://doi.org/10.5194/nhess-2019-200
Preprint. Discussion started: 28 June 2019

Natural Hazards and Earth System Sciences
Open Access
Discussions

In this context early warning systems (EWS) play a key role. UNISDR (2009) defines early warning systems as "the set of capacities needed to generate and disseminate timely and meaningful warning information to enable individuals, communities and organizations threatened by a hazard to prepare and to act appropriately and in sufficient time to reduce the possibility of harm or loss". A complete EWS is divided into four steps: (1) risk knowledge, (2) monitoring, forecasting and warning, (3) communication of an early warning system and (4) response capability [UN, 2006]. The first two steps are related to the field of physical sciences while the two last steps are associated to social science aspects. There are several works related to the impact of the early warning system in the prevention of floods. Baudoin et al. (2014) and UNISDR (2015) show some interesting examples on how early warning systems can save lives and reduce the damage to the people. Borga et al. (2011) developed an early warning system methodology for flash floods in Europe through the HYDRATE project. The authors enhance the capability of flash flood forecasting in ungauged basins by exploiting the extended availability of flash flood data and the improved process understanding. Alfieri et al. (2012) analyse several early warning systems applied to detect surface water flooding, flash floods, debris flows, land-slides induced by extreme rainfall events, river and coastal floods. The authors proposed several tasks to palliate the main drawbacks of some of these systems. Also, Hossain et al. (2014) and Cools et al. (2012) where a satellite-based forecast system is applied to measure the water depth of the river at the "Valley of Death" and an early warning system to detect flash flood is developed to the Sinai Peninsula, respectively. In Europe a very interesting example of an early warning system is the EWS applied to the region of Flanders (Schelfaut et al., 2012 and CIW, 2013). In this work, the different steps are analysed under the FREEMAN project (Flood REsilience Enhancement and MANagement). The European Flood Awareness System (EFAS) is also another example of an EWS developed to the sponsorship of the European Commission. This system provides daily streamflow forecast for Europe starting from up to 10-days weather forecast (medium-term forecast). More details of this model can be shown in Thielen et al. (2009), Pappenberger et al. (2011), Cloke et al. (2013) and Alfieri et al. (2014). Using this model Dottori et al. (2017) develop a methodology to adapt EFAS to real time forecasting. Demerit et al. (2013) analyse the problems derived from the use of the early warning system to medium and long-term flood forecast, mainly the dissemination of the information to people potentially affected by these events. They reveal that flood forecasters usually wait the confirmation from local institutions

(Hydrologic Confederations…) instead of acting based on the information provided by the early warning systems. These local systems are focused in short-term forecast (0 to 48 h) that are more suitable to evacuation than fore damage mitigation. The latter is associated to the long and medium-term forecasts provided by the European early warning systems.

In this paper, a flood early warning system based on precipitation forecast is presented. The system, which is being developed in collaboration with the Hydrographic Confederation of Miño-Sil River, consists of three steps: i) precipitation forecast; ii) use of a hydrologic model to detect extreme flows; iii) use of a hydraulic model that is applied at certain areas only under extreme flows. Starting from 1-day, 2-day and 3-day precipitation forecast windows provided by the Regional Meteorological Office (MeteoGalicia), the outflows associated to the catchment of the Miño River (NW Spain) were obtained using the HEC-HMS model (U.S. Army Corps of Engineers, 2018). This model was previously calibrated for the area of study by means of series of historical flood events detected over the last decade. The numerical model Iber (Bladé et al., 2014) was used to obtain water depth and velocity under extreme flow conditions for some risk areas where previous events have caused damages or material loses. Both models (i.e., HEC-HMS and Iber) are freely available software so the system can be applied at any location without costs derived from the licences of commercial codes.

The paper, which aims to describe the steps followed to develop the EWS, is organized as follows. First, a description of the area of study (the upper reach of Miño River and the city of Lugo, NW Spain) is shown. Then the methodology to obtain the weather forecast, the computation of the run-off and the hydraulic processes are briefly presented. Also the communication among all the models (Precipitation Forecast - Run-Off - Hydraulic processes) is explained. Next, the results of the precipitation and outflow forecast of a series of historical flood events are presented along with a statistic analysis of their accuracy. Finally, the numerical water depth obtained for a particular flood event at the city of Lugo is shown and compared with field data measured during the event.

2. Study area

The area of study is located in north-western Spain (Figure 1). It corresponds to the upper reach of the Miño River. This catchment area is about 2200 km^2 and the elevation ranges

https://doi.org/10.5194/nhess-2019-200
Preprint. Discussion started: 28 June 2019

from 360 to 980 m.a.s.l. The average annual precipitation ranges from 144 to 1300 mm year^{-1}.

Figure 1 (upper-left panel) shows the catchment of the upper reach of the Miño River, which is divided into three main sub-basins according to their topographic characteristics. Seven rain gauges operated by MeteoGalicia are located in the entire catchment. Table 1 shows the location and the elevation of each of the rain gauges located in the upper reach of the Miño River. The outlet of this catchment is located in the city of Lugo (Figure 1, lower panel). This area is usually flooded during the events of extreme precipitations in the upper reach of the Miño River. The absence of dams in the catchment to regulate the flow also affect the high frequency of these events.

3. Methodology

In this work, an automatic EWS is proposed. This system is composed of several elements as shown in Figure 2. All these components are orchestrated by a Python script that is the responsible of gather and transform the data properly in order to feed the models used in the system. First of all, the rainfall forecast performed with the Weather Research and Forecasting model is provided by the weather agency (MeteoGalicia). Details are provided in next section. Forecasted data are automatically downloaded and the rainfall relative to each sub-basin is extracted to fed the hydrological model HEC-HMS. When the catchment outflow obtained with HEC-HMS surpasses the 90th percentile of historical data, it is considered as a possible extreme event and the following steps will be applied. In that case, this outflow will be used as inlet condition for the hydraulic simulation using the model Iber+ to provide flood maps with water depths and velocities at certain risk areas (the city of Lugo in this particular case). Data provided by Iber+ are processed for hazard evaluation. At this stage the system checks if there is a risk condition in the areas accessible by pedestrians. These areas are user defined and can be changed depending on seasonal events. In order to emit a warning alert, the criteria of Cox et al. (2010) are used to define safety limits for children since they are the most vulnerable population group. Following this criterion, a warning will be emitted if there is a zone where any of the following thresholds are surpassed: the water depth (h) is higher than 0.5 m, the water velocity (v) is higher than 0.2 ms^{-1} or the product ($h \cdot v$) excess 0.4 m^{2}s^{-1}. This warning is sent in form of report to a decision maker, so an expert can validate the resulting data and discard false positives.

https://doi.org/10.5194/nhess-2019-200
Preprint. Discussion started: 28 June 2019

Natural Hazards and Earth System Sciences
Open Access
Discussions

The details of the components of the EWS, the data sources, and the calibration processes are shown in the following sections.

3.1 Precipitation data

3.1.1 Forecasted precipitation data

Forecasted precipitation data were obtained from the Regional Meterological Office (MeteoGalicia, http://www.meteogalicia.gal/). MeteoGalicia publishes weather forecast results based on the Weather Research and Forecasting (WRF) Model (Skamarock et al., 2005) (http://www.wrf-model.org). The WRF model is a numerical weather prediction system at regional mesoscale designed mainly for forecasting applications. WRF is run operationally since 2008 providing daily data until the end of 2012 (00 UTC) and twice a day (00 UTC and 12 UTC) from then on, with a 72- hour forecast window, a temporal resolution of 1 hour and maximum spatial resolution of 4 km (Sousa et al., 2013). Data provided by MeteoGalicia are freely available at its THREDDS (Thematic Realtime Environmental Distributed Data Service) server, also maintaining an historical archive of past forecast since 2008. The model outputs provide several variables related to weather. In the case of this study, precipitation information was automatically obtained for the areas under interest at the 00 UTC of each day during the period 2008-2018.

3.1.2 Measured precipitation data

Real precipitation data at hourly scale were obtained from the rain gauges managed by MeteoGalicia, which is responsible of their maintenance and data quality control. Data from these rain gauges will be used to assess the performance of the MeteoGalicia Weather Forecast to predict extreme rain events. The rain gauges selected for this study were shown in Figure 1 and their location and elevation is detailed in Table 1.

3.2 River discharge data

Daily discharge data of the Minho River were provided by the corresponding river Basin Authority (Confederación Hidrográfica del Miño-Sil, https://www.chminosil.es). In this case of study, Miño flow data at Lugo station covering the period 2008-2018 were selected. River data were used to calibrate and validate the hydrologic model system used during the development of this study.

https://doi.org/10.5194/nhess-2019-200
Preprint. Discussion started: 28 June 2019

3.3 HEC-HMS & Iber+

Here the hydrological and hydraulic models used in the study will be briefly described along with the methods to analyze their accuracy.
The distributed model HEC-HMS (Feldman, 2000 and U.S. Army Corps of Engineers, 2018) was used to analyse the rain-runoff processes and the numerical code Iber (Bladé et al., 2014) was used to compute the hydraulic processes.
The HEC-HMS is a model developed by the US Army Corps of Engineers that is applied to simulate continuous hydrological processes. The HEC-HMS model can be used to analyse various hydrological aspects, such as flooding events, reservoir capacity, stormwater warnings, and stream restoration (U.S. Army Corps of Engineers 2008). HEC-HMS is divided into four components: (i) an analytical model: calculation of direct runoff and channel routing; (ii) a basin model: representation of hydrological elements in a watershed; (iii) a system to manage input data and store data; (iv) a post-processing tool to report and illustrate simulation results.
Taylor diagrams (Taylor, 2001) were used to compute the accuracy of the results obtained with HEC-HMS by means of the normalised standard deviation (Eq. 1), centred root-mean square difference (Eq. 2) and correlation (Eq. 3).

$$\sigma_{n,A} = \frac{\sqrt{\frac{\sum_{i=n}^{N}(A_i-\bar{A})^2}{N}}}{\sigma_B} \quad (1)$$

$$E_{n,A} = \frac{\sqrt{\frac{\sum_{i=n}^{N}[(A_i-\bar{A})-(B_i-\bar{B})]^2}{N}}}{\sigma_B} \quad (2)$$

$$R_A = \frac{\sum_{i=n}^{N}[(A_i-\bar{A})(B_i-\bar{B})]}{N\,\sigma_A\,\sigma_B} \quad (3)$$

where A is a numerical variable and B a reference variable. The subscript i refers to the different samples, N is the number of samples, barred variables refer to mean values and σ is the standard deviation.
The hydraulic simulations were carried out using the numerical model Iber (Bladé et al. 2014). Iber is a numerical code that solves the 2D Shallow Water Equations by means of finite volume schemes (FVS). The software package is formed by three elements: pre-

https://doi.org/10.5194/nhess-2019-200
Preprint. Discussion started: 28 June 2019

processing tool, numerical model and post-processing tool. The first and the last modules are based in the software GID (GID, 2018). It provides a user friendly graphical interface (GUI) to create the case and edit the parameters that define the problem to solve. It also provides tools to analyse the results of the numerical simulations. The pre-processing and post-processing tools were used only during the modelling and testing of the study area. However, the automatic EWS runs the model in batch mode without user interaction. Iber was recently improved in terms of efficiency becoming Iber+ (García-Feal et al. 2018). This new parallel implementation of the Iber model takes advantage of GPU computing using the Nvidia CUDA (NVIDIA CO., 2019) platform. Using this technology, the new implementation is able to run up to 100 times faster. This fact makes Iber+ especially suitable for the implementation of an EWS where the response times can be crucial to issue an early alert. The accuracy of the water depth results computed with Iber+ at several control points was assessed by means of the *bias* and the *RMSE* (Root Mean Square Error) relative to the values measured *in situ* during the extreme event recorded on January 2013.

4. Results and discussion

4.1 Accuracy of MeteoGalicia Precipitation Forecast

The capability of MeteoGalicia Weather Forecast system to predict rain events was evaluated by means of the comparison with real precipitation data provided by the rain gauges in the area of study. For that purpose, the predicted (numerical) precipitation was obtained at the closest grid points to the location of the rain gauges. The correlation between predicted and measured precipitation was calculated for each rain gauge during the available period (2008-2018). For this calculation, Spearman rank correlation was used due to its robustness to deviations from linearity, as well as its strength to the influence of outliers. This procedure was carried out for 3 forecast windows (1-24 h, 25-48 h and 49-72 h; 1-day, 2-day and 3-day forecast from now on) to determine the accuracy of the forecast at different temporal scales.

The values of the correlation for each rain gauge are shown in Table 2. In general, precipitation prediction offers a good representation of the registered values. In fact, correlations above 0.8 were obtained for the first two windows (1-day and 2-day forecast),

https://doi.org/10.5194/nhess-2019-200
Preprint. Discussion started: 28 June 2019

although with a higher correlation for the first one. The correlation is slightly lower for the 3-day forecast, although it is still close to 0.8.

Therefore, it can be concluded that the precipitation forecast provided by MeteoGalicia offers results very close to the real rain events for the entire time series of precipitation data (2008-2018). This shows the accuracy of MeteoGalicia models to forecast precipitation events up to three days in advance.

4.2 Calibration and validation of hydrological processes using HEC-HMS

A set of 15 extreme flood events registered during the period 2008-2018 were used to calibrate and validate the rain-runoff model HEC-HMS by comparing the outflows measured at the gauge station located at Lugo with the flows obtained with HEC-HMS using the 1-day forecast of precipitation.

Calibration was carried out using the specific calibration tools implemented in HEC-HMS (Feldman, 2000) in order to choose two independent parameters, the curve number (CN) and lag time (L_g), for each sub-basin of the domain. Eleven flood events were used for calibration purposes and the rest of cases were used to validate the model. Table 3 shows the values of the CN and L_g for each sub-basin obtained for each event used in the calibration step.

The mean values of CN and L_g of each sub-basin were used to validate the model in four flood events (01/2013, 01/2014, 02/2016 and 03/2018) by means of a Taylor diagram (Figure 3).

The values of normalised standard deviation range from to 0.8 to 1.2, the values of the root mean squared difference range from 0.3 to 0.6 and the correlation of the numerical results range from to 0.85 to 0.95. These values show that the mean values of CN and L_g obtained in the calibration step characterise the behaviour of the basin with a high accuracy.

Figure 4 compares the numerical and measured streamflow for the event that happened in January 2013 using the three forecast windows. The left panel shows that time series of the flows predicted by the model are similar to those measured at the gauge station. The right panel is the Taylor diagram corresponding to the three forecast windows. The standard deviation is observed to range from 0.8 to 1.2 for the three forecasts. RMSD values for 1-day and 2-day forecasts are around 0.3, being around 0.6 for the 3-day forecast. Finally, the correlation coefficient for 1-day and 2-day forecasts are close to 0.95, being around 0.85 for the 3-day forecast.

https://doi.org/10.5194/nhess-2019-200
Preprint. Discussion started: 28 June 2019

4.3 Case of study

Once the predicted water flow showed to reproduce the real events with a high accuracy (E_n ~ 0.8, σ_n ~ 0.3 and R ~ 0.95), the water depth and velocity during the flood event that affected Lugo on 20th January, 2013 were computed using the numerical code Iber+ (Garcia-Feal et al., 2018). Figure 5 shows the numerical domain at Lugo, where seven land uses were defined to model the characteristics of the terrain. The Manning's coefficient associated to each land use are shown in Table 4. Figure 5 also shows the location of the inlet and outlet boundary conditions.

The topography of the area of study was obtained from raster files freely downloaded from the Instituto Geográfico Nacional website (https://www.ign.es/web/ign/portal). The computational domain was discretised using a mesh with near 200,000 unstructured triangular elements, with an average area of 2 m^2.

Five control points were defined at the area of study (see Figure 6) to analyse the accuracy of the numerical results. Points from 1 to 4 are located in places next to the riverbank usually frequented by pedestrians while the last one is located in the riverbed. Therefore, the first four points are of special interest to issue an alert.

Figure 7 shows the values of the water depth obtained in the numerical simulations along with the water depth measured at the control points during the flood event. The range of the values of the numerical water depths correspond to 3 times of the standard deviation of the values obtained from the 12 p.m. to 4 p.m. of January 20th, 2013 and the dot corresponds to the mean value of the water depth during the range of hours defined. Visually, the numerical results are quite similar to the field data when considering the 1-day forecast, especially if one considers that the accumulation of the small inaccuracies of the three models involved can give rise to biases. The values are slightly less accurate when considering the 2-day forecast and worse for the 3-day forecast due to lower accuracy in rainfall forecast.

Table 5 shows the values of the *bias* and the *RMSE* between measured and computed water elevations using the three different forecast windows. The minimum values of *bias* and *RMSE* are obtained with the 24h forecast (0 and 21 cm, respectively). The accuracy decreases with the forecast window, although results are still good for a 2-day forecast and acceptable for a 3-day forecast. The *RMSE*, which is a measure of the deviation from real values, was calculated for the three forecast windows being smaller than 0.5 m, which is the critical height indicated by Cox et al. (2010). Especially remarkable is the

https://doi.org/10.5194/nhess-2019-200
Preprint. Discussion started: 28 June 2019

simulation obtained with 1-day forecast, with a deviation of just 21 cm respect to real data and a null *bias*. The good agreement between the measured and computed values indicates that the system can be used to issue alert up to 3 days in advance.

Figure 8 shows the maximum water depth and maximum velocity obtained for 1-day forecast. Hazard maps (Figure 9) can be computed from these data according to the criterion of Cox et al. (2010). Several recreation areas near the riverbanks show to have surpassed the aforementioned hazard threshold. Therefore, decision-makers can use the map to restrict activities in these areas, in order to mitigate the consequences of floods.

5. Conclusions

In this paper an Early Warning System for flood prediction using precipitation forecast was presented. This system starts automatically using rain forecast data retrieved from Regional Meteorological Office (MeteoGalicia) and concatenates two freely available software packages (HEC-HMS and Iber+). The upper reach of the Miño River (NW Spain) and, in particular, the city of Lugo were used as a benchmark.

A Python script was developed to deal with all the components involved in the system without user interaction. First, the precipitation forecast provided by MeteoGalicia is automatically obtained for the area of study. Second, rain forecast is provided to HEC-HMS as an input to compute the streamflow in the catchment area. When the streamflow obtained with HEC-HMS surpasses the 90th of the historical percentile at some previously selected risk area (the city of Lugo in this particular case), the possibility of an extreme event is detected and that streamflow is automatically defined as an inlet condition for Iber+. Finally, data obtained from Iber+ are processed for risk assessment and, if applicable, decision makers are reported.

The accuracy of the different models was assessed to analyse the capability of the system to provide reliable results. First, the accuracy of the precipitation forecast provided by MeteoGalicia was analysed for the period 2008-2018 showing that the 1-day forecast is slightly more accurate than the 2-day forecast, being the 3-day slightly worse, although the three forecast windows showed a reasonable agreement with field data. As a second step, the accuracy of HEC-HMS to reproduce extreme flows was assessed by means fifteen flood events recorded over for the period 2008-2018. Taylor diagrams were used to compute the accuracy of the numerical streamflow compared with field data obtained at the control station located near Lugo. Once again, results were satisfactory for the three

https://doi.org/10.5194/nhess-2019-200
Preprint. Discussion started: 28 June 2019

Natural Hazards and Earth System Sciences Discussions

forecast windows, especially for the 1-day and 2-day forecast. Finally, a historical flood event recorded in January, 2013 was used to assess the accuracy of Iber+ to reproduce real water elevation at 5 control points located at the riverbank and riverbed. Both the *RMSE* and the *bias* between the measured and computed elevations were satisfactory, especially for the 1-day forecast.

The system needs less than 1 hour to run the models for a 3-day forecast horizon. While data can be downloaded in a few seconds and the hydrologic model can be run in less than a minute, no matter the extent of the area, the real bottleneck in the system is the hydraulic model. Fortunately, the execution time does not necessarily increase with the number of risk areas since different areas can be run concurrently when the available hardware resources allow it. Taking into account that meteorological data are available every day at 5:00 a.m. the system can provide an alert report to decision makers before 6:00 a.m. Additional improvements can be applied without additional cost in term of runtime. For example, an ensemble approach can be applied when rain forecasts from different sources are used as an input condition for HEC-HMS, in such a way that Iber+ is only executed when at least one of the hydrological realizations indicates a possible extreme event.

Additional research is still needed to cover the entire Miño river basin, where other problems may arise from the presence of dams. The system, when fully developed, can even help to manage dams intelligently, maximizing energy production and dampening floods at the same time.

The Early Warning System can be easily adapted for any area of the world since the required input data can be obtained freely from public institutions and the models to compute the hydrological and the hydraulic processes (HEC-HMS and Iber+, respectively) are both freely available. Therefore, the EWS is especially interesting for developing countries where the acquisition of commercial software is not sustainable.

Code and data availability. Freely available data and software (HEC-HMS and Iber+) were used for this work. The detailed processing flowchart is shown in Fig. 2 (Section 3 – Methodology).

Author contributions: JGC, OGF and DFN designed the research, conducted the analysis and wrote the paper, ; JMDA and MGG supervised the research and revised the paper.

Competing interests. The authors declare that they have no conflict of interest.

Acknowledgements

This work was partially supported by Water JPI-WaterWorks Programme under project Improving Drought and Flood Early Warning, Forecasting and Mitigation (IMDROFLOOD, code: PCIN-2015-243), and by Xunta de Galicia under Project ED431C 2017/64-GRC "Programa de Consolidación e Estructuración de Unidades de Investigación Competitivas (Grupos de Referencia Competitiva). We especially thank Carlos Ruiz del Portal Florido, Head of the Hydrological Planning Office, Hydrographic Confederation of Miño-Sil River for helpful discussions and for providing access to real data within the context of INTERREG-POCTEP Programme project RISC_ML (Code: 0034_RISC_ML_6_E).

References

Alfieri, L., Salamon, P., Pappenberger, F., Wetterhall, F., and Thielen, J.: Operational early warning systems for water-related hazards in Europe, Environ. Sci. Policy, 21, 35-49, https://doi.org/10.1016/j.envsci.2012.01.008, 2012.

Alfieri, L., Pappenberger, F., Wetterhall, F., Haiden, T., Richardson, D., and Salamon. P.: Evaluation of ensemble streamflow predictions in Europe, J. Hydrol., 517, 913–922, https://doi.org/10.1016/j.hydrol.2014.06.035, 2014.

Alfieri, L., Bisselink, B., Dottori, F., Naumann, G., de Roo, A., Salamon, P., Wyser, K., and Feyen, L.: Global projections of river flood risk in a warmer world, Earth's Future, 5 (2), 171-182,. https://doi.org/10.1002/2016EF000485, 2017.

Baudoin, M., Henly-Shepard, S., Fernando, N., Sitati, A., and Zommers, Z.: Early warning systems and livelihood resilience: exploring opportunities for community participation, UNU-EHS Working Paper Series, No.1, United Nations University Institute of Environment and Human Security (UNU-EHS), Bonn, 2014.

Bladé, E., Cea, L., Corestein, G., Escolano, E., Puertas, J., Vázquez-Cendón, E., Dolz, J., and Coll, A.: Iber -River modelling simulation tool [Iber: herramienta de simulación numérica del flujo en ríos], Revista Internacional de Metodos Numericos para Calculo y Diseno en Ingenieria, 30 (1), 1-10. https://doi.org/10.1016/j.rimni.2012.07.004, 2014.

Borga, M., Anagnostou, E. N., Blöschl, G., and Creutin, J. D.: Flash flood forecasting, warning and risk management: The HYDRATE project, Environ. Sci. Policy, 14 (7), 834-844, https://doi.org/10.1016/j.envsci.2011.05.017, 2011.

CIW, Rapport Globale Evaluatie Overstromingen, Report in Dutch [Evaluation Report for Floods] Committee for Integrated Water Resources Management (CIW), Flemish Authority, Brussels, Belgium, 2013.

Cloke, H., Pappenberger, F., Thielen, J., and Thiemig, V.: Operational European flood forecasting, in: Environmental Modelling: Finding Simplicity in Complexity, 2nd ed., Wainwright, J. and Mulligan, M. (Eds.), John Wiley and Sons, Ltd, Chichester, UK. https://doi.org/10.1002/9781118351475.ch25, 2013.

Cools, J., Vanderkimpen, P., El Afandi, G., Abdelkhalek, A., Fockedey, S., El Sammany, M., Abdallah, G., El Bihery, M., Bauwens, W., and Huygens, M.: An early warning system for flash floods in hyper-arid Egypt, Nat. Hazard Earth Syst. Sci., 12 (2), 443-457, https://doi.org/10.5194/nhess-12-443-2012, 2012.

Cox, R. J., Shand, T. D., and Blacka, M.J.: Australian Rainfall and Runoff revision project 10: appropriate safety criteria for people, Water Res., 978, 085825-9454, 2010.

Dankers, R., and Feyen, L.: Climate change impact on flood hazard in Europe: An assessment based on high-resolution climate simulations". J. Geophys. Res-Atmos., 113 (19), https://doi.org/10.1029/2007JD009719, 2008.

Demeritt, D., Nobert, S., Cloke, H. L., and Pappenberger, F.: The European Flood Alert System and the communication, perception, and use of ensemble predictions for operational flood risk management, Hydrol. Process., 27 (1), 147-157, https://doi.org/10.1002/hyp.9419, 2013.

Dottori, F., Kalas, M., Salamon, P., Bianchi, A., Alfieri, L., and Feyen, L.: An operational procedure for rapid flood risk assessment in Europe, Nat. Hazards Earth Syst. Sci., 17 (7), 1111-1126. https://doi.org/10.5194/nhess-17-1111-2017, 2017.

Feldman, A.D.: Hydrologic Modeling System HEC-HMS, Technical Reference Manual, p. 157. Institute for Water Resources Davis, USA, 2000.

García-Feal, O., González-Cao, J., Gómez-Gesteira, M., Cea, L., Domínguez, J.M., Formella, A.: An accelerated tool for flood modelling based on Iber, Water, 10 (10), art. no. 1459, https://doi.org/10.3390/w10101459, 2018.

GID Reference Manual. https://www.gidhome.com/, 2018

Hossain, F., Siddique-E-Akbor, A. H. M., Yigzaw, W., Shah-Newaz, S., Hossain, M., Mazumder, L. C., Ahmed, T., Shum, C. K., Lee, H., Biancamaria, S., Turk, F. J., and Limaye, A.: Crossing the "valley of Death": Lessons learned from implementing an operational satellite-based flood forecasting system, B. Am.Meteorol. Soc., 95 (8), 1201-1207, https://doi.org/10.1175/BAMS-D-13-00176.1, 2014.

Jonkman, S. N.: Global perspectives on loss of human life caused by floods, Nat. Hazards, 34 (2), 151-175, https://doi.org/10.1007/s11069-004-8891-3, 2005.

Noji, E. K.: The public health consequences of disasters, Prehospital and disaster medicine : the official journal of the National Association of EMS Physicians and the World Association for Emergency and Disaster Medicine in association with the Acute Care Foundation, 15 (4), pp. 147-157, 2000.

NVIDIA Corporation. CUDA C Programming Guide. Available online: https://docs.nvidia.com/cuda/pdf/CUDA_C_Programming_Guide.pdf

Pappenberger, F., Thielen, J., and Del Medico, M.: The impact of weather forecast improvements on large scale hydrology: analysing a decade of forecasts of the European Flood Alert System, Hydrol. Process., 25, 1091–1113, https://doi.org/10.1002/hyp.7772, 2011.

Schelfaut, K., Pannemans, B., van der Craats, I., Krywkow, J., Mysiak, J., and Cools. J.: Bringing flood resilience into practice—the FREEMAN project, Environ. Sci. Policy, 14 (7), 825-833, https://doi.org/10.1016/j.envsci.2011.02.009, 2012.

Skamarock, W. C. , Klemp, J. B., Dudhia, J., Gill, D. O., Barker, D. M., Wang, W., and Powers, J. G.: A Description of the Advanced Research WRF Version 2. Tech. Rep., National Center for Atmospheric Research, 2005.

Sousa, M.C., Alvarez, I., Vaz, N., Gomez-Gesteira, M., and Dias, J. M.: Assessment of wind pattern accuracy from the QuikSCAT satellite and the WRF model along the Galician coast (Northwest Iberian Peninsula), Mon. Weather Rev., 141 (2), 742-753, https://doi.org/10.1175/MWR-D-11-00361.1, 2013.

Taylor, K.E.: Summarizing multiple aspects of model performance in a single diagram, J. Geophys. Res., 106, 7183-7192, 2001

Thielen, J., Bartholmes, J., Ramos, M. H., and De Roo, A.: The European flood alert system-part 1: Concept and development, Hydro. Earth Syst. Sc., 13 (2), 125-140, https://doi.org/10.5194/hess-13-125-2009, 2009.

https://doi.org/10.5194/nhess-2019-200
Preprint. Discussion started: 28 June 2019

UNISDR. UNISDR terminology on disaster risk reduction. United Nations Office for Disaster Risk Reduction, 2009.
UNISDR. Making development sustainable: the future of disaster risk management. Global Assessment Report on Disaster Risk Reduction, United Nations Office for Disaster Risk Reduction (UNISDR), Geneva, Switzerland, 2015.
UN, Global survey of early warning systems, A report prepared at the request of the Secretary-General of the United Nations, 2006.
U.S. Army Corps of Engineers. Hydrologic Modeling System (HEC-HMS) Applications Guide: Version 3.1.0. Davis: Institute for Water Resources, Hydrologic Engineering Center. 2008.
U.S. Army Corps of Engineers, Hydrologic Modeling System (HEC-HMS) User's Manual: Version 4.3. Institute for Water Resources Davis: Hydrologic Engineering Center, 2018.

Figure Captions

Figure 1. Area of study. The rain gauges (rg_1, …,rg_7) located in the catchment (upper-left panel) and the area of study in Lugo (lower panel) are also shown. (PNOA courtesy of © Instituto Geográfico Nacional).
Figure 2. Flowchart of the proposed EWS.
Figure 3. Taylor diagram of the validation cases (01/2013, 01/2014, 02/2016 and 03/2018).
Figure 4. Time series of the outflow at the control point obtained in the gauge station (dashed line) and calculated using the three forecast windows (left panel) and Taylor diagram for the same cases (right panel).
Figure 5. Numerical domain at Lugo. The land uses and the location of the boundary conditions (red lines) are also shown. (PNOA courtesy of © Instituto Geográfico Nacional).
Figure 6. Location of the five control points at the area of study in Lugo. (PNOA courtesy of © Instituto Geográfico Nacional).
Figure 7. Comparison between water depth (*h* in meters) between the numerical model (.) and the field data (x) for the three forecast windows 1-day (left), 2-day (middle) and

https://doi.org/10.5194/nhess-2019-200
Preprint. Discussion started: 28 June 2019

3-day (right). The range of the numerical values correspond to 3 times the standard deviation of the elevations obtained from the 12 a.m. to 4 p.m. of January 20th, 2013.

Figure 8. Maximum water depth (upper panel) and maximum velocity (lower panel) obtained with Iber+ for the 1-day precipitation forecast. (PNOA courtesy of © Instituto Geográfico Nacional).

Figure 9. Areas where hazard criterion is surpassed. (PNOA courtesy of © Instituto Geográfico Nacional).

Table 1. Location and elevation of the rain gauges located in the area of study (The system of reference for latitude and longitude is the EPSG: 4326).

Table 2. Values of the correlation (Spearman's r) of the precipitation forecast using the measured data as reference at each rain gauge. The averaged values for each precipitation forecast are also shown.

Table 3. Curve number (*CN*) and lag time (L_g) values for each sub-basin for different flood events. The mean value and the standard deviation are provided in lower rows.

Table 4. Manning's coefficients of the numerical domain.

Table 5. Values of the *RMSE* and *bias* for three forecast windows.

https://doi.org/10.5194/nhess-2019-200
Preprint. Discussion started: 28 June 2019

Table 1. Location and elevation of the rain gauges located in the area of study (The system of reference for latitude and longitude is the EPSG: 4326).

Rain gauge id.	Name	Latitude	Longitude	Elevation (m.a.s.l.)
rg_1	Labrada	43.4054	-7.50205	662
rg_2	Lanzós	43.3746	-7.64468	470
rg_3	Guitiriz-Mirador	43.2266	-7.78307	684
rg_4	Sanbreixo	43.1457	-7.79112	496
rg_5	Castro de Rei Lea	43.1559	-7.48588	428
rg_6	Pol	43.1626	-7.28258	647
rg_7	Corno do Boi	43.0374	-7.89265	731

Table 2. Values of the correlation (Spearman's r) of the precipitation forecast using the measured data as reference at each rain gauge. The averaged values for each precipitation forecast are also shown.

	Forecast window (h)		
Rain gauge	1-24	25-48	49-72
rg_1	0.84	0.82	0.77
rg_2	0.84	0.82	0.79
rg_3	0.83	0.81	0.77
rg_4	0.81	0.79	0.75
rg_5	0.81	0.80	0.76
rg_6	0.84	0.83	0.79
rg_7	0.83	0.81	0.77
Mean value	0.83	0.81	0.77

Table 3. Curve number (CN) and lag time (L_g) values for each sub-basin for different flood events. The mean value and the standard deviation are provided in lower rows.

	Sb_1		Sb_2		Sb_3	
Date of the flood event	CN	L_g (min)	CN	L_g (min)	CN	L_g (min)
12/09	92	1154	97	2700	98	2770
11/10	80	1140	84	2702	80	2781
03/13	79	1157	96	2701	99	2774
11/13	80	1148	86	2685	83	2778
01/14	78	1155	96	2700	98	2767
03/14	81	1153	88	2706	92	2764
01/15	96	1153	99	2701	99	2773
03/15	81	1151	91	2700	98	2771
02/16	81	1155	88	2700	98	2767
03/16	82	1153	80	2711	84	2764
03/18	80	1152	82	2691	93	2769
Mean	85	1152	90	2700	93	2771
σ	6	4	6	7	7	5

https://doi.org/10.5194/nhess-2019-200
Preprint. Discussion started: 28 June 2019

Table 4. Manning's coefficients of the numerical domain.

Land's uses	Manning's coefficient ($s\ m^{-1/3}$)
River	0.025
Brush	0.050
Trees	0.120
Sparse vegetation	0.080
Infrastructure	0.020
Industrial	0.100
Residential	0.150

Table 5. Values of the *RMSE* and *bias* for three forecast windows.

	RMSE (cm)	*bias* (cm)
1-day	21 ± 5	0 ± 5
2-day	28 ± 6	4 ± 6
3-day	41 ± 5	-35 ± 5

https://doi.org/10.5194/nhess-2019-200
Preprint. Discussion started: 28 June 2019

Natural Hazards and Earth System Sciences
Discussions

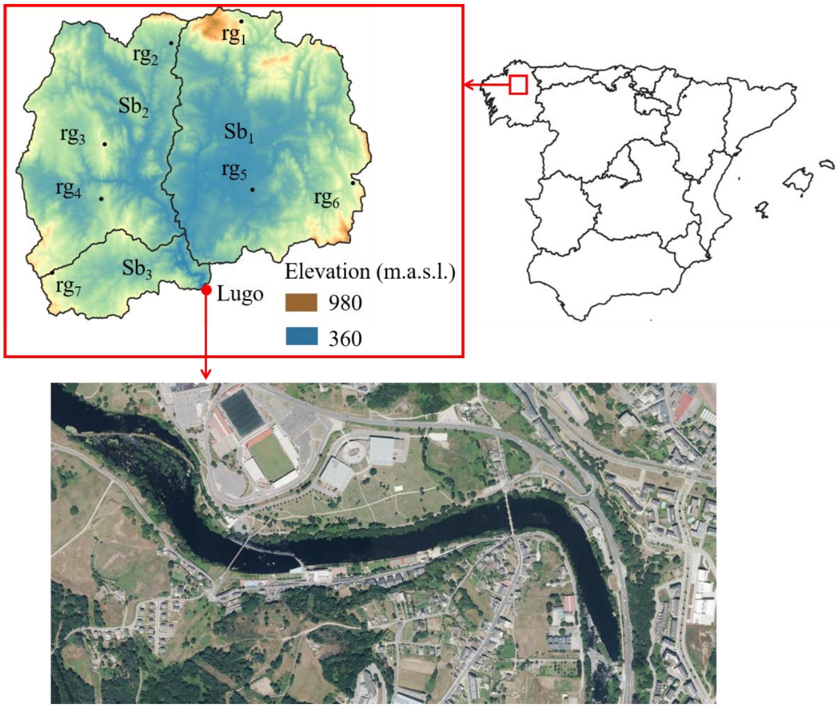

536

537

538 **Figure 1.** Area of study. The rain gauges (rg_1, …,rg_7) located in the catchment (upper-
539 left panel) and the area of study in Lugo (lower panel) are also shown. (PNOA courtesy
540 of © Instituto Geográfico Nacional).

541

542

543

544

545

https://doi.org/10.5194/nhess-2019-200
Preprint. Discussion started: 28 June 2019

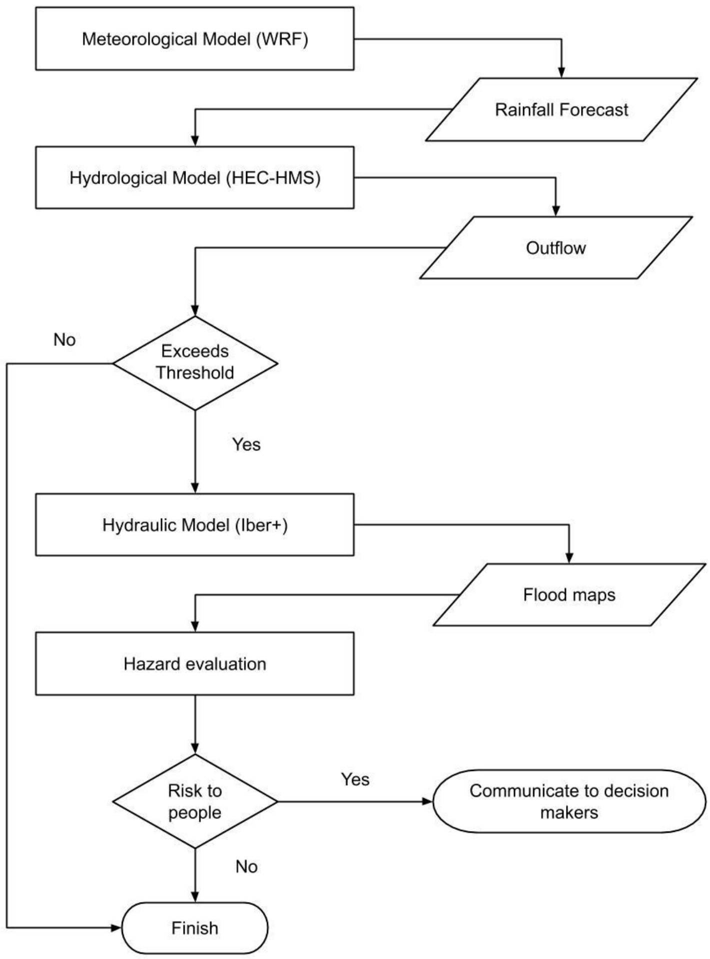

Figure 2. Flowchart of the proposed EWS.

https://doi.org/10.5194/nhess-2019-200
Preprint. Discussion started: 28 June 2019

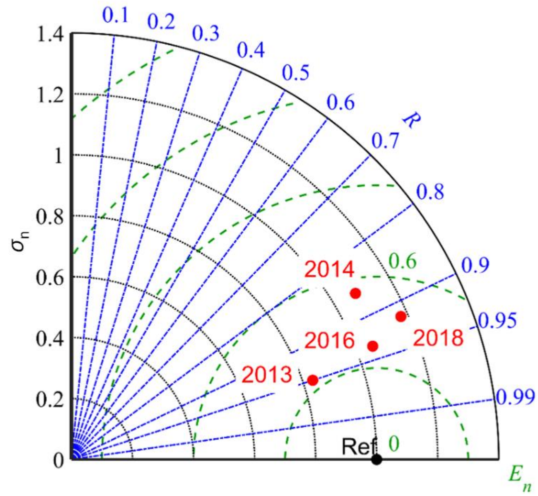

Figure 3. Taylor diagram of the validation cases (01/2013, 01/2014, 02/2016 and 03/2018).

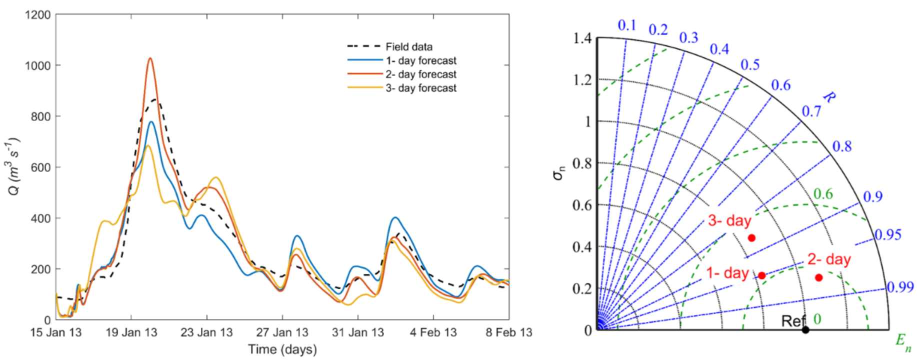

Figure 4. Time series of the outflow at the control point obtained in the gauge station (dashed line) and calculated using the three forecast windows (left panel) and Taylor diagram for the same cases (right panel).

https://doi.org/10.5194/nhess-2019-200
Preprint. Discussion started: 28 June 2019

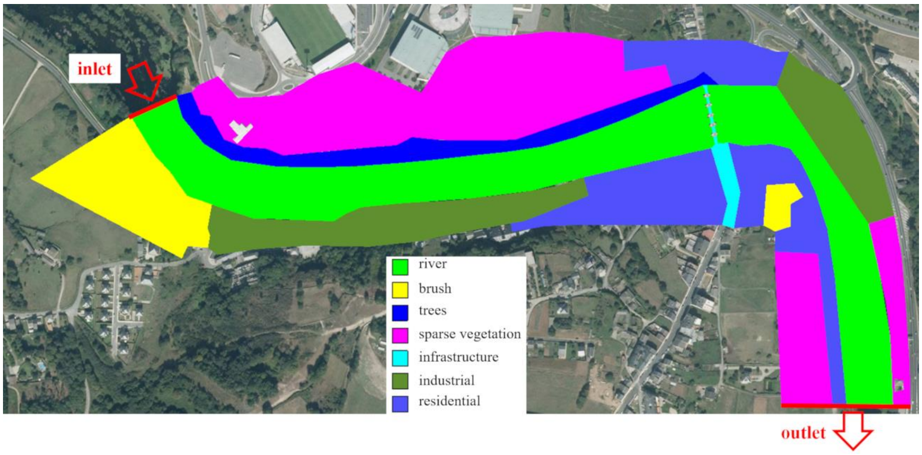

Figure 5. Numerical domain at Lugo. The land uses and the location of the boundary conditions (red lines) are also shown. (PNOA courtesy of © Instituto Geográfico Nacional).

Figure 6. Location of the five control points at the area of study in Lugo. (PNOA courtesy of © Instituto Geográfico Nacional).

https://doi.org/10.5194/nhess-2019-200
Preprint. Discussion started: 28 June 2019

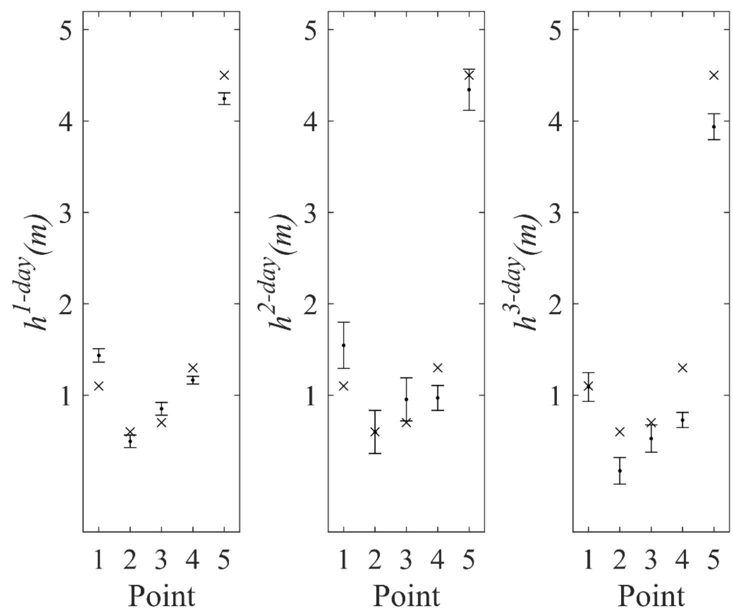

Figure 7. Comparison between water depth (*h* in meters) between the numerical model (.) and the field data (x) for the three forecast windows 1-day (left), 2-day (middle) and 3-day (right). The range of the numerical values correspond to 3 times the standard deviation of the elevations obtained from the 12 a.m. to 4 p.m. of January 20th, 2013.

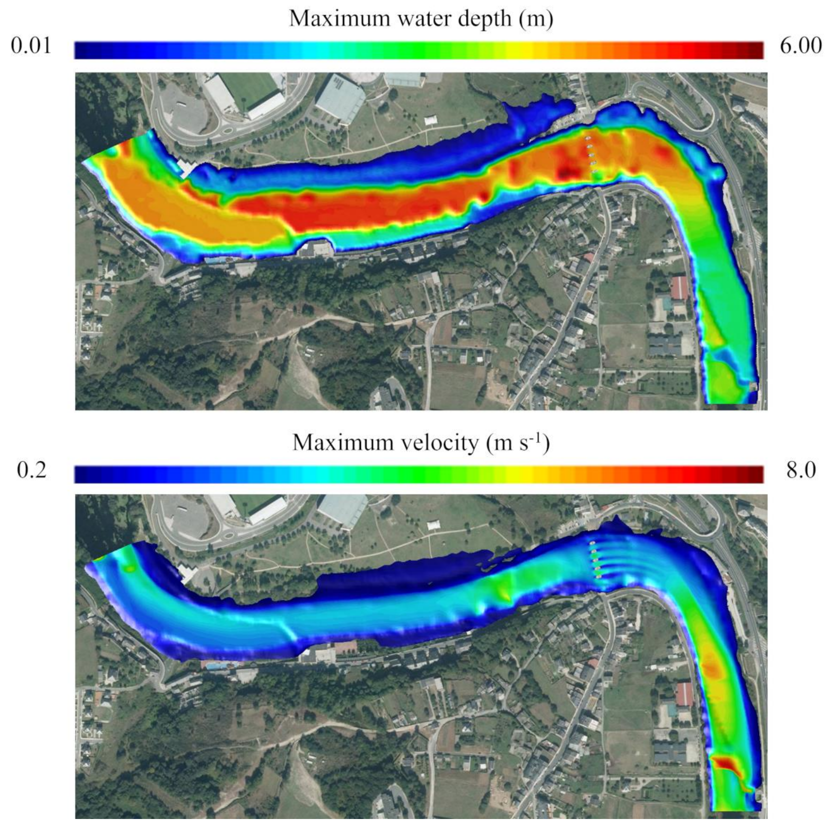

Figure 8. Maximum water depth (upper panel) and maximum velocity (lower panel) obtained with Iber+ for the 1-day precipitation forecast. (PNOA courtesy of © Instituto Geográfico Nacional).

https://doi.org/10.5194/nhess-2019-200
Preprint. Discussion started: 28 June 2019

Natural Hazards and Earth System Sciences
Open Access
Discussions

Figure 9. Areas where hazard criterion is surpassed. (PNOA courtesy of © Instituto Geográfico Nacional).